Aerodynamic Design of the Scaled Supersonic Experimental Airplane

Yuichi Shimbo+, Kenji Yoshida+, Toshiyuki Iwamiya‡, Ryoji Takaki‡
National Aerospace Laboratory
7-44-1, Jindaiji-higashi machi, Chofu, Tokyo 182-8522, Japan
and
Kisa Matsushima*
Fujitsu Limited
1-9-3, Nakase, Mihama-ku, Chiba-shi, Chiba 261-0023, Japan

Abstract

As a part of the NAL's scaled supersonic experimental airplane program to establish an aerodynamic design system based on Computational Fluid Dynamics (CFD), an aerodynamic configuration with no propulsion system was designed in a two-stage process. First, a baseline configuration was designed using a conventional linear theory. Then, the CFD and a supersonic inverse method were used to refine the wing geometry and to achieve a higher lift-to-drag ratio at a design point of M=2 and CL=0.1. A non-linear effect such as body to wing interference and a wing thickness effect were also handled in this phase. By making use of the inverse method, an upper surface of the wing was designed aiming at a natural laminar flow with a flat-type pressure distribution to reduce a friction drag. A wing warp was also adjusted to achieve an optimal load distribution designed by the linear theory to reduce a pressure drag. The designed new wing was evaluated by a Navier-Stokes analysis and an incompressible boundary layer stability code (SALLY code) and was found to have an improved lift-to-drag ratio, with a wider laminar flow regime and smaller friction drag than the initial geometry. Finally, the CFD analysis was compared with supersonic wind tunnel data and was found to be a well validated tool to be used in the design.

1. Introduction

Thirty years after the Concord was designed based on a linear theory and an extensive use of wind tunnel tests, Computational Fluid Dynamics (CFD) techniques have made rapid progress enough to be incorporated in an aerodynamic design in aerospace industries. In order to play an important role in a worldwide cooperative program of developing a next generation supersonic airplane in early twenty-first century, the National Aerospace Laboratory (NAL) in Japan has been working on a scaled supersonic experimental airplane project since 1995 (Ref. 1). Two types of unmanned experimental airplanes are to be designed and the main goal of the project is to establish an aerodynamic design system based on the CFD and to validate it by flight tests of the designed vehicles. The first type of the experimental airplane is a clean configuration without any propulsion system and its goal is to establish a design system making full use of the CFD and an inverse method. Then, the second type with two jet engines is to be designed to establish a design optimization technique for a complete airplane configuration, including an engine/airframe integration problem. This paper summarizes the aerodynamic design process of the first one, which is planned to be flight tested in the year 2001.

2. Design Process

The aerodynamic design process was consisted of two stages. First, a baseline configuration was designed using a conventional linear theory. Then in the second stage, the CFD and a supersonic inverse method were fully used to refine the wing geometry and to improve a lift-to-drag ratio (L/D).

The design point was set to M=2 and CL=0.1, which was a typical cruise condition for an expected next generation SST. The outline of a complete aircraft configuration is shown in Fig. 1, along with four design concepts incorporated in the design. They are (1) Planform design, (2) Warped wing, (3) Area-ruled body and (4) Natural laminar flow (NLF) wing.

2.1 Linear Theory Design - Baseline Configuration

Planform Design

The wing of the baseline configuration was designed as a pure wing. An arrow wing with a subsonic leading edge at the design Mach number of two, and an aspect ratio ranging from 1.8 to 2.2 was examined as a candidate planform. Ninety-nine planforms with an identical area and a various combination of sweptback angles of an inner wing and an outer wing were generated and then, a drag-due-to-lift parameter K defined by eq. (1) of each

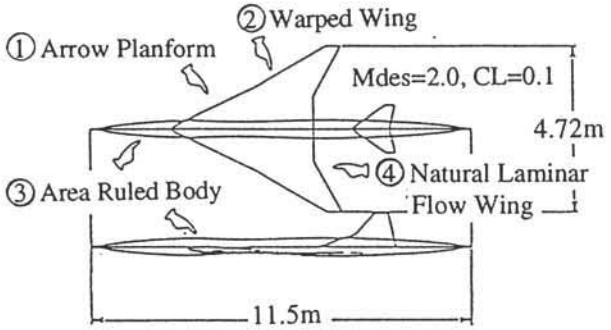

Fig. 1 Design Concepts Incorporated in the Design

+ Advanced Aircraft Research Group
‡ Computer Science Division
* Supercomputer System Engineering Division

planform was evaluated as a flat plate wing using a supersonic lifting surface theory. Finally eight planforms with lower K values were picked up for the next step.

$$CD = CDo + K(CL - CLo)^2 \quad (1)$$

where
CDo = Minimum drag
CLo = CL at CDo

Warp Design

For each of the eight wing planform selected from ninety-nine, a wing warp was designed using the Carlson's method (Ref. 2). The method designed an camber surface, zc(x,y), and an optimal load distribution

$$\Delta Cp(x,y) = Cp,lower(x,y)-Cp,upper(x,y) \quad (2)$$

which minimized the drag due to lift at the design point. Fig. 2 shows the result of the warp design. A planform with an aspect ratio of 2.2 and 66.0/61.2 deg inner/outer leading edge sweptback angles was finally selected as a baseline planform. Then, a thickness distribution of NACA 4 digit series airfoil was added to the camber surface to generate a baseline wing geometry. The thickness ratio was set to be 3.7% at a wing centerline and 3% at a wing tip.

Area-ruled Body Design

A supersonic area rule (Ref. 3) was applied to minimize a drag due to volume of the complete aircraft configuration. The cross-sectional area distribution was computed for the Sears-Haack body under M=2 and a necessary body length and volume condition. Then, the body of revolution was designed by subtracting an equivalent cross-sectional area of the wing and tails from the one of the Sears-Haack body. The tails and a wing location were determined by referring to a database of similar SST both in operation and in a conceptual design phase. The body behind an empennage looks rather long in Fig. 1, because there needs a room for a parachute system to be used in a recovery phase of the flight test.

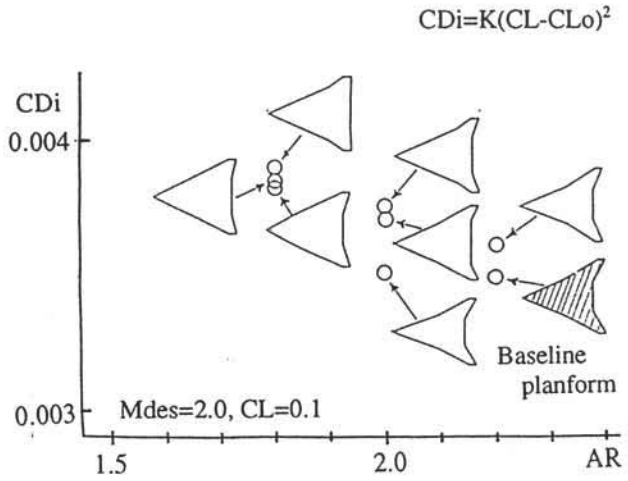

Fig. 2 CDi Evaluation of the Warped Planforms

2.2 CFD and Inverse Method Design - Refinement to a NLF Wing

CFD Analysis of the Baseline Configuration

The baseline wing-body configuration was analyzed at M=2 by a Navier-Stokes code developed in house at NAL (Ref. 4) and the results were compared with one of the linear theory. The CFD analysis was usually conducted at α=0, 2, 5 deg and then one more angle of attack corresponding to CL=0.1 was added. The drag polar of the CFD analysis in Fig. 3(a) shows a loss in CLo, the lift coefficient at minimum pressure drag. Fig. 3(b) shows an iso-load contour of the linear design (Left) and the CFD analysis (Center) at CL=0.1, along with the contour of the difference between them (Right). The hatching in the right figure corresponds to a region where the load computed by the CFD is smaller than one by the linear theory and a load deficit near the leading edge, especially at inner wing is obvious. Both findings indicate the warp effect designed by the linear theory is lost in the CFD analysis, due to a non-linear effect of a wing thickness and an interference with the body.

Quasi-Inverse Design

Following the findings above, a recovery of the warp effect, in other words, a recovery of the optimal load distribution designed by the linear theory was taken up as the first strategy to reduce the pressure drag at the design point. A simple quasi-inverse method was developed for this purpose, and from here on, the target load distribution of the wing-body configuration computed by Mitsubishi Heavy Industries, Ltd. (MHI) was used instead

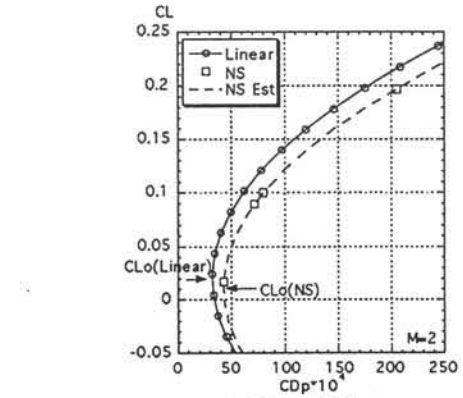

(a) Drag Polar

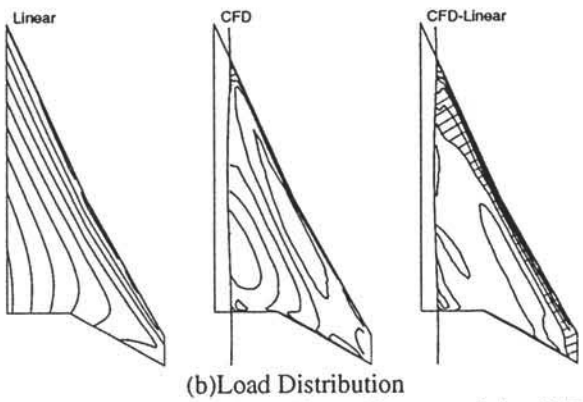

(b)Load Distribution

Fig. 3 Comparison of the Linear Theory and the CFD

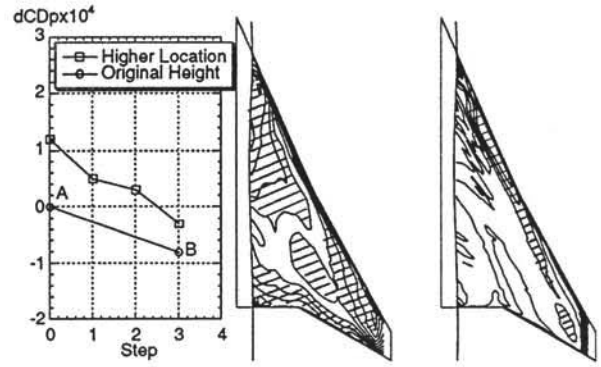

(a) Drag Evaluation (b)Load Distribution

Fig. 4 Results of the Quasi-Inverse Design

of one of the pure wing configuration. The quasi-inverse method picked up wing sections every 5% semispan location and treated each of them as an independent airfoil. The difference between the target load distribution and the CFD result were converted into an increment in a slope of the camber line at each chordwise location using a supersonic small disturbance theory (Ref. 5). Then, a new camber line was computed by integrating the new camber line slope. After completing the quasi-inverse design at all spanwise locations, a new wing was defined by adding the original thickness distribution to the new camber line and was put into the CFD analysis for the drag evaluation. Fig. 4(a) shows a drag reduction effect at two wing height relative to the body. At a higher wing location, the drag at the design point increased from one of the original height, but it turned to decrease with a gradual change of the geometry. At the original height, the drag also decreased even by a rapid change of the geometry which was equivalent to the three steps of the higher wing case. In Fig. 4(b), the hatching indicates the region where the deviation from the target load distribution is greater than 0.01 in ΔCp and it clearly shows the effectiveness of the quasi-inverse method and the refinement strategy.

Natural Laminar Flow Wing Concept

For the scaled supersonic experimental airplane with a body length of only 11.5m, the Reynolds number is rather small comparing with a full scale SST, and the friction drag reaches about a half of the total drag in case the flow over the airplane is assumed to be full turbulent. Therefore, a natural laminar flow concept was introduced as the second strategy of the wing refinement to reduce the friction drag and to improve L/D.

For a wing with a large sweptback angle as one used for a SST, a crossflow (CF) instability is a trigger of the laminar to turbulent transition as well as the Tollmien-Schlichting (TS) instability. The crossflow instability comes from a spanwise pressure gradient in a direction normal to a local streamline and it tends to glow fast near the leading edge where the static pressure changes very rapidly.

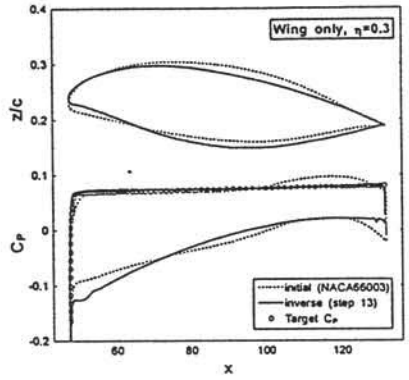

(a) Geometry and Pressure Distribution

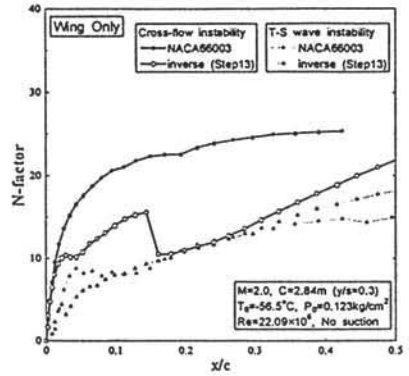

(b) Evaluation of the Amplification Factor

Fig. 5 Effect of the Flat Pressure Distribution (Ref. 6)

After a temporary second configuration was defined by changing the airfoil section of the baseline (NACA 4-digit series) to a laminar flow airfoil (NACA 66 series), a target pressure distribution on the upper surface aiming at the natural laminar flow was defined by Kawasaki Heavy Industries, Ltd. (KHI). To minimize the growth of the CF instability, the target has a rapid pressure drop near the leading edge and a flat chordwise pressure distribution toward the trailing edge (Ref. 6). A pure wing with this target pressure distribution was designed by KHI as an example case and the transition characteristics were evaluated by the SALLY code described later (Fig. 5). It showed a smaller amplification factor of the disturbance both for the CF and TS instabilities, which indicated a wider laminar region than the temporary second configuration.

Inverse Design

Given a target pressure distribution, the inverse method mathematically provides an increment of the geometry to be modified from the original. In NAL, a transonic inverse method had been developed and mainly applied to an aerodynamic design of wings for commercial airplanes (Refs. 7, 8). A supersonic version of the inverse method was newly developed in a cooperative research program between NAL and the Tohoku University (Ref. 9). In this method, a panel method for a pure wing configuration was used to convert the pressure difference from the target into the increment of the geometry.

Fig. 6 summarizes a flowchart of the inverse design. The target pressure on the upper surface was a flat-type distribution defined by KHI aiming at the natural laminar flow. The lower surface pressure distribution was then set by subtracting the optimal load distribution defined by MHI from the upper surface pressure distribution. It should be noted that the two refinement strategies proved in Figs. 4 and 5 were combined to reduce both the pressure drag and the friction drag.

The temporary second configuration with NACA 66 series airfoil sections was used as an initial geometry of the inverse design. The increment of the geometry computed by the inverse method was added to the original at 14 spanwise locations with a certain relaxation and a weak constraint for a maximum wing thickness ratio. Then, a new wing geometry was defined using the three-dimensional geometry generation software CATIA and was evaluated by the CFD. It took about a week to complete the whole one iteration of the inverse design. After ten iterations, the wing configuration was fixed to a final third configuration.

3. Evaluation of the Design

3.1 Pressure Drag

The solid lines in Fig. 7(a) show typical airfoil geometries and pressure distributions of the third configuration at the design point, along with the initial geometry of the inverse design (dashed lines) and the target (dots). At each spanwise location, the pressure distribution of the third configuration shows better agreement with the target than the initial geometry. As for the load distribution, Fig. 7(b) shows the deviation from the optimum in the same manner as Fig. 4(b) and the third configuration clearly shows an improvement. From these figures, it is confirmed that the inverse method successfully changed the wing geometry toward a favorable direction. Regarding the integrated pressure drag, the minimum pressure drag CDpo was improved because the inverse method relaxed the leading edge droop to recover the load deficit. However, the drag-due-to-lift parameter K of the third configuration increased at the same time and in total, the pressure drag itself did not change much from the initial geometry of the inverse design (Table 1).

3.2 Friction Drag

The friction drags of both the third and the temporary second configuration were evaluated at η=0.3 and 0.7 using an incompressible boundary layer stability code (SALLY code) based on the e^N method (Ref. 10). This code could treat a wing with a sweptback angle and take both the TS and CF instabilities into account. Given an airfoil geometry, a pressure distribution on the upper surface and the Reynolds number of each spanwise location, the amplification factor N of the disturbance with various frequencies was evaluated assuming the pressure distribution was all the same at any spanwise location. For each of the TS and CF instability, the overall amplification factor of the disturbance was defined as an envelope of the result for each frequency. Then, once a critical value of N was specified, the chordwise transition point was determined as the cross point of the envelope and the critical N value, Ncr.

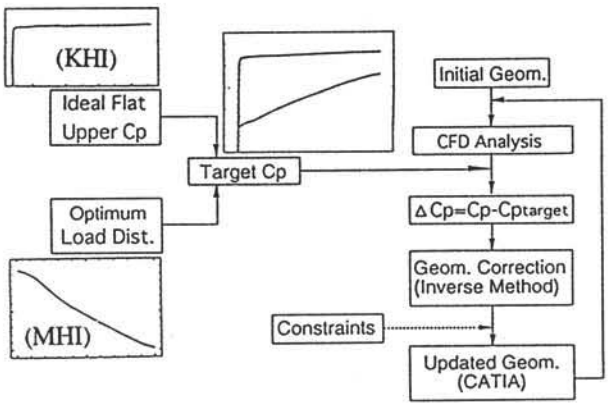

Fig. 6 Flowchart of the Inverse Design

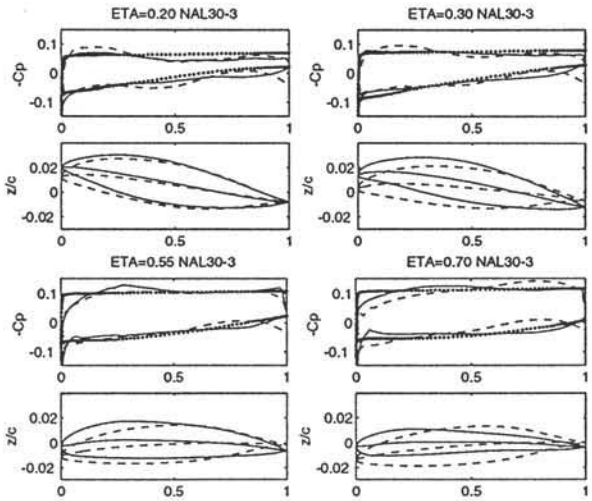

(a) Geometries and Pressure Distributions

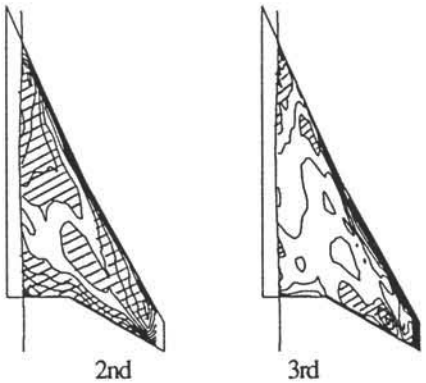

(b) Load Distribution

Fig. 7 CFD Results of the Third Configuration

Table 1 Evaluation of the Pressure Drag

	2nd	3rd
CLo	0.0110	0.0116
CDpo(*1)	42.7	41.6
K	0.4666	0.4823
CDp@CL=0.1	79.7	79.3

(*1) Drag is evaluated in count (1 count is 0.0001 in CD)

Fig. 8 shows a close-up of the pressure distribution near the leading edge and the results of the SALLY code analysis only for the CF instability. Assuming Ncr to be 20 ~ 25 at an altitude of 10 to 18 km expected in the flight test of the experimental airplane, the transition due to the CF instability at η=0.3 was expected at x/c=0.11 for the temporary second configuration (Table 2). As for the third configuration, the envelope did not reach Ncr because the pressure distribution around the leading edge was modified very well toward the target pressure distribution. However, it did not necessarily mean a full laminar flow, and instead, a transition due to the TS instability was assumed at around x/c=0.5. At η=0.7, the pressure distribution was not close enough to the target and therefore, the envelopes of both configurations had slight difference and the transition due to the CF instability was expected at x/c=0.31. As a reference, the target pressure distribution was also evaluated and the transition at x/c=0.5 due to the TS instability was assumed because no transition due to the CF instability was found.

A drag reduction factor defined by

$$\frac{\text{section friction drag with a transition at (x/c)tr}}{\text{section friction drag with a full turbulent flow}}$$

was computed at these two spanwise locations to evaluate the improved transition characteristics. Here, friction drag coefficients of both laminar and turbulent boundary layers were ones on a flat plate at the flight Reynolds number of the experimental airplane, and a full turbulent flow was assumed on the lower surface. Then, the total wing friction drag was estimated by assuming the drag reduction factor at η=0.3 represented the whole inner wing (inner part of the leading edge kink at η=0.5045) and one for η=0.7 represented the whole outer wing. As a result, the total wing friction drag of the third configuration decreased about 4 count (1 count is 0.0001 in CD) from the second configuration. Although the transition location did not change at η=0.7, the drag penalty comparing with the target pressure distribution was only one count because the exposed area of the outer wing was much smaller than the inner wing.

Table 2 Evaluation of the Friction Drag of the Wing

Item	η	2nd	3rd	Target
Transition location (x/c)tr	0.3	0.11	0.50	0.50
	0.7	0.31	0.31	0.50
Drag Reduction Factor	0.3	0.95	0.76	0.76
	0.7	0.85	0.85	0.77
Total CDfw(*1)		30.6	26.4	25.4

(*1) Drag is evaluated in count (1 count is 0.0001 in CD)

Table 3 Evaluation of the Overall Drag at CL=0.1

Item	2nd	3rd
Pressure Drag CDp(*1)	79.7	79.3
Friction Drag CDf(*1)	63.5	59.3
Total Drag CD(*1)	143.2	138.6
L/D	7.0	7.2

(*1) Drag is evaluated in count (1 count is 0.0001 in CD)

3.3 Overall Characteristics

Evaluated as the complete aircraft configuration, the total drag of the third configuration was improved by about 5 counts from the initial geometry of the inverse design. It

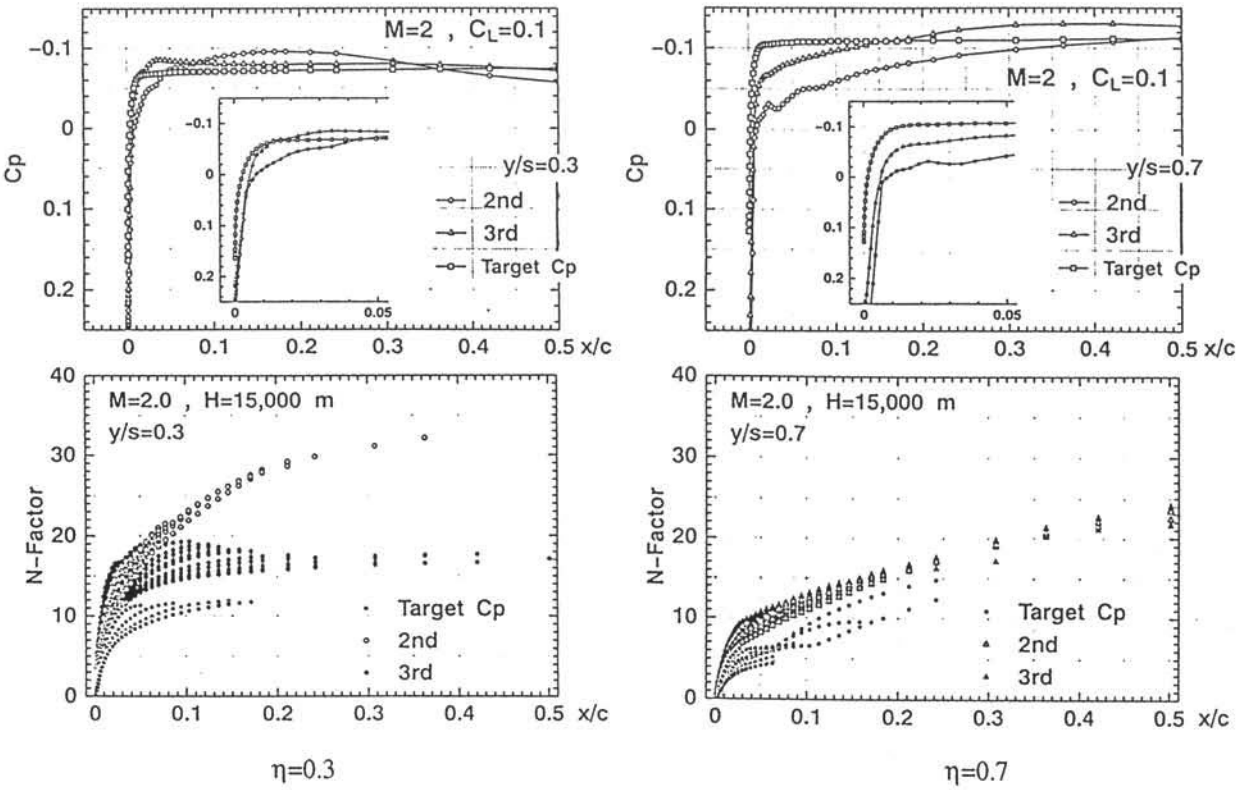

η=0.3 η=0.7

Fig. 8 Evaluation of the Transition Characteristics

led to an increase in L/D from 7 to 7.2 (Table 3), indicating the validity of the inverse design and the two strategies taken up in the second stage of the aerodynamic design.

4. Comparison with the Wind Tunnel Data

Two types of 8.5% scale wind tunnel models of the complete aircraft configuration were fabricated and tested at the 1m supersonic wind tunnel at NAL. The first one was for a force measurement and mounted by a straight sting through a six-component internal balance. Another was for a pressure measurement and was equipped with 90 pressure taps arranged on the body and three spanwise locations of the wing. The transition point of the wing was fixed at x/c=0.03 for both models because the Reynolds number was much smaller than the flight environment. Fig. 9(a) shows the comparison of the lift characteristics of the wing-body configuration at M=2. Both the absolute value of CL and the lift slope of the wind tunnel test show very good agreement with the Navier-Stokes analysis. Fig. 9(b) shows the drag polar of the wing-body configuration, with the apex of a parabolic fitting adjusted to an origin of the plot. The drag-due-to-lift parameter K is almost identical but slightly larger in CFD. As for the pressure distribution measured in the complete aircraft configuration, Fig. 9(c) shows the comparison at η=0.3 and 0.7 at the design point of M=2 and CL=0.1. The agreement between the wind tunnel test and the CFD is also very well and it is found that the CFD analysis used in the design procedure is a quite reliable tool to evaluate the aerodynamic design. However, a farther evaluation is still necessary about the transition characteristics on the upper surface of the wing.

5. Conclusions

The aerodynamic configuration of the NAL's scaled supersonic experimental airplane with no propulsion system was designed in the two-stage process. First, the baseline configuration was designed using the linear theory. Then it was refined using the CFD and the inverse method, aiming at a natural laminar flow on the upper surface and the optimal load distribution designed by the linear theory. The Navier-Stokes analysis and the incompressible boundary layer stability code (SALLY code) analysis showed the designed new wing had better transition characteristics and an improved friction drag by about 4 counts, leading to an increase in the lift-to-drag ratio by 0.2. In addition, the CFD analysis was compared with supersonic wind tunnel data and was found to be a well validated tool to be used in the design. However, a farther evaluation is still necessary about the transition characteristics on the upper surface of the wing.

Acknowledgment

The authors express special thanks to the Kawasaki Heavy Industries, Ltd. and the Mitsubishi Heavy Industries, Ltd. for their cooperative efforts to the whole design process.

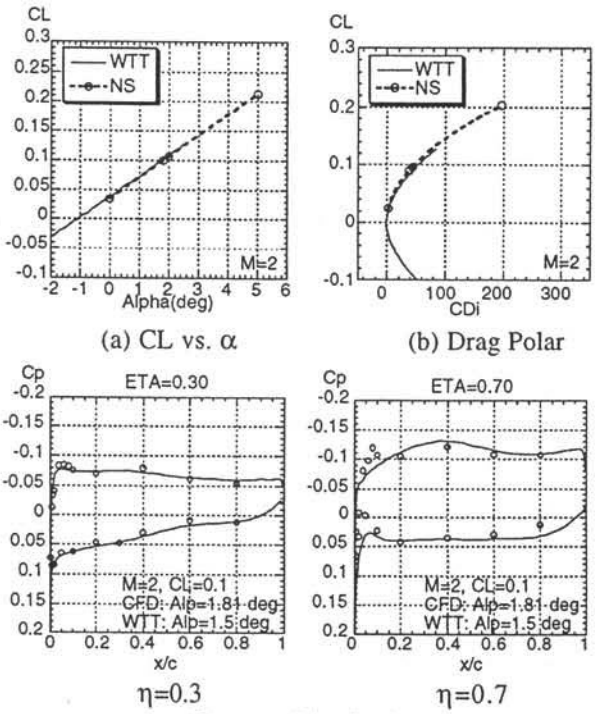

(a) CL vs. α (b) Drag Polar

(c)Pressure Distribution

Fig. 9 Comparison with the Wind Tunnel Test

References

(1) Sakata K., SST Research Project at NAL, 1st International CFD Workshop on Supersonic Transport Design, Tokyo, Mar., 1998

(2) Carlson H. W. and Miller D. S., Numerical Method for the Design and Analysis of Wings at Supersonic Speeds, NASA TN D-7713, 1974

(3) Ashley H. and Landahl M., Aerodynamics of Wings and Bodies, Addison-Wesley Publishing Company, Inc., 1965

(4) Takaki R., Iwamiya T. and Aoki A., CFD Analysis Applied to the Supersonic Research Airplane, 1st International CFD Workshop on Supersonic Transport Design, Tokyo, Mar., 1998

(5) Shimbo Y., Yoshida K., Iwamiya T. and Takaki R., Linear and Non-Linear Analysis/Design of a SST Configuration, Proc. of the 29th Fluid Dynamics Conference, Sapporo, Sep., 1997 (in Japanese)

(6) Ogoshi H., Aerodynamic design of an Supersonic airplane wing - Application of the Natural Laminar Flow concept to Airfoil, Proc. of the 47th Nat. Cong. of Theoretical & Applied Mechanics, Jan., 1998 (in Japanese)

(7) Takanashi S., Iterative Three-Dimensional Transonic Wing Design Using Integral Equations, J. of Aircraft, Vol. 22, No. 8, pp. 655-660, 1985.

(8) Tatsumi S. and Takanashi S., Experimental Verification of Three Dimensional Transonic Inverse Method, AIAA-85-4077, Oct., 1985

(9) Jeong S., Matsushima K., Iwamiya T., Obayashi S. and Nakahashi K., Inverse Design Method for Wings of Supersonic Transport, AIAA 98-0602

(10) Srokowski, Mass Flow Requirements for LFC Wing Design, AIAA 77-1222